ACCURATE FABRICATION OF ALIGNED NANOFIBERS *VIA* A DOUBLE-NOZZLE NEAR-FIELD ELECTROSPINNING

by

Guojie XU[a], Han WANG[a*], Zhifeng WANG[a], Jiarong ZHANG[a], Rouxi CHEN[b], Ziming ZHU[a], Xindu CHEN[b**], YaJu LIN[a], Yixiang ZHAO[c***], Jianting LI[c], Meixi CHEN[a], Yang LI[a], Zhengyi XIN[a], and Hongxin LIN[a]

[a] Guangdong Provincial Key Laboratory of Micro-Nano Manufacturing Technology and Equipment, Guangdong University of Technology, Guangzhou, China
[b] South China University of Technology, Guangzhou, Guangdong, China
[c] Guanzhou Medical University, Guangzhou, Guangdong, China

The near-field electrospinning is considered as one of the most effective techniques to direct-write aligned fibers which can be applied to various high-tech areas, including energy harvester, tissue engineering, and wearable sensors. For large area aligned pattern printing, the multi-nozzle electrohydrodynamic printing is an efficient method to enhance productivity. As a branch of electrohydrodynamic printing technology, the near-field electrospinning is a crucial concern to make an investigation for the formation of aligned nanofibers. Here we fabricated various nanostructures from beaded fibers to aligned fibers and crimped fibers by the double-nozzle near-field electrospinning process. We found three key parameters affecting the process, including the collector speed, the applied voltage, and the electrode-to-collector distance, and the collector speed is the key factor affecting the crimped frequency. This paper provides a reliable experimental basis and theoretical guidance for the multi-nozzle near-field electrospinning to accurately direct-write microfibers and nanofibers.
Key words: *near-field electrospinning, double-nozzle, aligned nanofibers, process, crimped fibers*

Introduction

Nanofibers/nanowires have superior electrical and physical properties due to their 1-D confined nanostructure, and they have been used in various applications including scaffolds for tissue engineering, optoelectronic devices, chemical transformation, wearable electronics, field-effect transistor, and others [1-7]. As the most effective technique to produce microfibers and nanofibers by appending a high voltage power to micro-scale flows, the electrospinning (ES) printing has been attracting more and more attention [8-10]. However, due to the chaotic whipping during the spinning process, the ES is unstable and uncontrollable to deposit accurately fibers [11].

In order to improve the controllability of fiber deposition and fiber morphology, Sun *et al.* firstly proposed the near-field electrospinning (NFES) in 2006 [11, 12], which was believed to be the most effective one, and has found wide applications to energy harvester, tissue

---

engineering, wearable sensors, microelectromechanical systems, *etc.* [13-16]. Chang *et al.* [17] used the NFES to obtain PVDF nanofibers film with great piezoelectric properties, and it was used to fabricate nanogenerators. In addition, Fuh [13] used biodegradable alginate fibers fabricated by the NFES to control cell orientation.

Although the NFES has obvious advantages, the drawback of low production efficiency is also obvious [11, 18, 19]. Therefore, it is a common requirement to increase its productivity in a simple and cost-effective way.

The production rate of the multi-nozzle ES method is several times higher than that of its single-needle partner [20, 21]. So, it is an efficient way to increase the number of spinnerets for mass production of nanofibers by NFES. However, there was almost no investigation on the interaction of the jets in multi-nozzle NFES. The double-nozzle NFES process is the best candidate for theoretical analysis. Pan *et al.* [22] fabricated parallel fibers by using a rotating double-nozzle with different distances, but it is unable to deposit fibers in a determinate distance. Moreover, Wang *et al.* [23] achieved controllable deposition and much denser aligned nanofibers by rotating the dual-nozzle setup.

In this paper, to study the relationship between various parameters and the deposition morphology, we present a dual-nozzle NFES process for fabricating aligned nanofibers with different process parameters, including the collector speed, the applied voltage, the electrode-to-collector distance. As a result, we make an exploration for the influence of various parameters on the structure and morphology of the aligned nanofibers during the deposition.
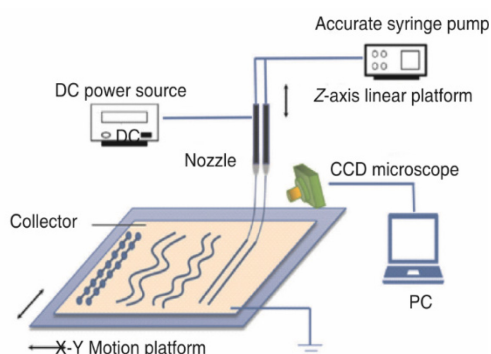
Figure 1. Double-nozzle NFES device and schematics

Materials and methods

Polyethylene oxide (PEO, $M_w = 2 \cdot 10^6$ g/mol) was purchased from Aladdin in China to prepare a polymer solution. The PEO nanofibers were direct-written using 5% (w/w) PEO solution with distilled water as solvent. The experimental NFES direct-writing device (QZNT-M08) was purchased from Foshan Lepton Precision Measurement and Control Technology Co., Ltd., and the principle is shown in fig. 1. Double nozzles were installed on z-axis linear platform and connected to a high voltage power source (DW-P503-1ACDF, Dongwen), while the collection plate was attached to the ground. A syringe pump with constant flow rate ($V_f = 0.2$ µm per minute) was to feed the spun solution into the double nozzle set-up. In addition, there was a charge-coupled device (CCD) microscope (DCR-HC 28, SONY) used to observe the movement of jets in the double-nozzle NFES process.

Results and discussion

This paper analyzed the relationship between various parameters and the structure of the deposition during NFES aligned pattern process using the double-nozzle system, by adjusting the collector speed, V_c, the applied voltage, U, and the electrode-to-collector distance, H. The controllable process of the double-nozzle system to produce aligned fibers is of both theoretical importance and practical guidance for accurately writing micro-nanometer structures.

Xu, G., *et al.*: Accurate Fabrication of Aligned Nanofibers *via* a Double-Nozzle …
THERMAL SCIENCE: Year 2019, Vol. 23, No. 4, pp. 2143-2150

2145

Effect of the collector speed on the
direct-write deposition structure

As observed in fig. 2, the collector speed had great effect on the deposition structure during the spinning process. Beaded fibers were observed, fig. 2(a), when the collector speed was sufficiently small (1 mm per second). In our experiment, the flow rate was kept unchanged, a lower collector speed implies that a higher volume of spun fluid will remain the moving jet. According to the minimal surface principle in the calculus of variations, the remnant fluid tends to form a sphere-like beads during the solidification process. As the collector speed increased up to 3 mm per second, fig. 2(b), crimped fibers were obtained. The crimping process occurs when an axially moving jet is subject to a transverse vibration. The crimp frequency is greatly affected by the jet speed and its temperature. According to [9, 10], the fundamental crimp frequency, see eq. (11) in [9].

$$\omega = \sqrt{\Pi - \frac{aV_c^2}{A} + \frac{b}{A}} \tag{1}$$

where V_c is the collector speed, A – the section area of the fiber, a, b, and Π – the functions of temperature, geometrical, and fluid parameters, respectively.

In view of the mass conversion:

$$A\rho V_c = Q \tag{2}$$

where ρ is the density of the jet and Q – the flow rate. Equation (1) can be written:

$$\omega = \sqrt{\Pi - \frac{a\rho V_c^2}{Q} + \frac{b\rho V_c}{Q}} \tag{3}$$

Equation (3) reveals that there is a threshold velocity for the maximal frequency, when the V_c is less than the threshold value, a higher collector speed results in a lower a lower crimp frequency, and when V_c tends to the threshold, the frequency becomes infinite small and smooth fibers can be obtained as shown in fig. 2. When collector speed reaches 30 mm per second, stable parallel fibers can be obtained, so the threshold value is near 30 mm per second. The collector speed plays an important role in controlling crimpled fibers.
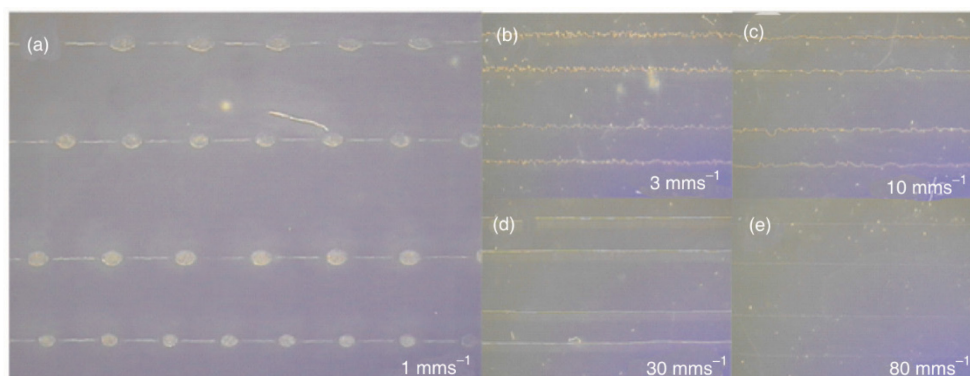
Figure 2. Jet deposition patterns at different collector speeds in the conditions with 0.5 inch needle length, 2.0 mm needle space, 4.0 mm electrode-to-collector distance
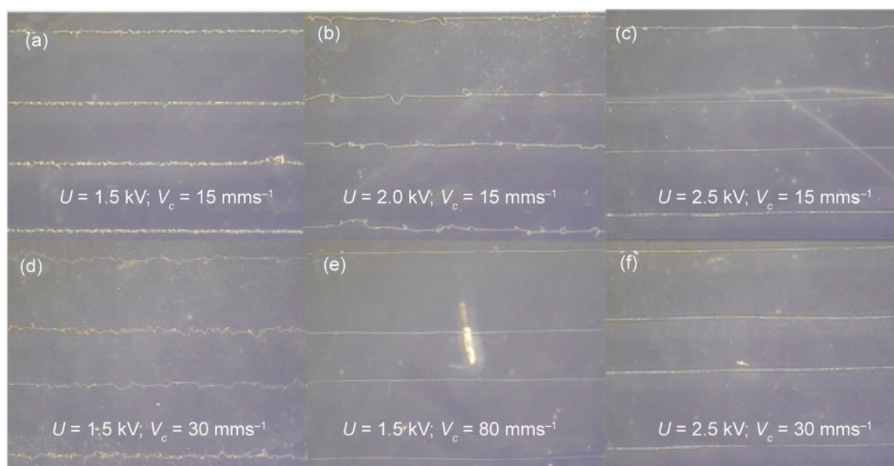(*for color image see journal web site*)
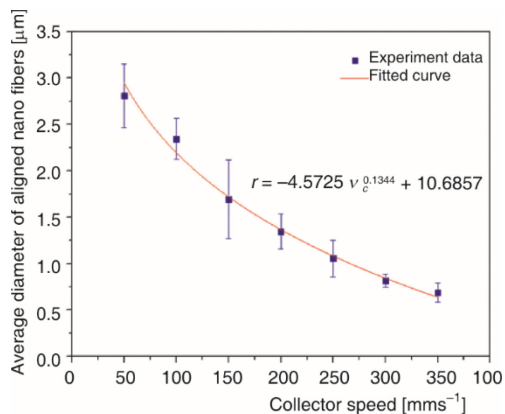
Figure 3. Average diameter of aligned nanofibers at different collector speeds

The collector speed affects greatly also the fiber diameter. As can be seen in fig. 3, when the collector speed increases from 50 mm per second to 350 mm per second, the average diameter of aligned nanofibers decreases from 2.81 μm to 0.78 μm.

Effect of applied voltage on the direct-write deposition structure

The applied voltage is the acting force in our experiment, a higher voltage results in a higher acceleration, as a result, a higher spinning velocity is predicted. According to the mass conservation, a higher velocity leads to smaller fiber diameters as shown in figs. 4 and 5.

Figure 4. The jets deposition pattern at different applied voltages; needle length: 0.5 inch, needle space: 2.0 mm, electrode-to-collector distance: 4.0 mm (*for color image see journal web site*)
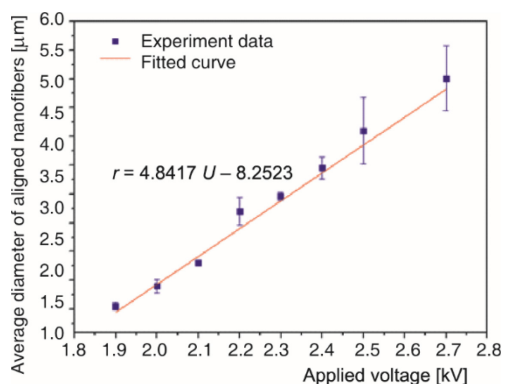
Figure 5. The average diameter of aligned nanofibers at different applied voltage

It can be clearly seen the crimping phenomenon is gradually observed when $u = 15$ mm per second and the applying voltage, U, increases from 1.5 KV to 2.5 KV as shown in figs. 4(a)-4(c). The jet maintains the stable parallel structure, and precipitates on the collector are in an aligned pattern when the collector velocity is 15 mm per second and the applied voltage is 2.5 KV. When the jet is deposited on the collector in a more elongated parallel pattern, fig. 4(f), when $u = 30$ mm per second, and the voltage becomes 2.0 KV.

Finally, the jets change from a Z-pattern slightly swinging to aligned nanofibers on the

Xu, G., *et al.*: Accurate Fabrication of Aligned Nanofibers *via* a Double-Nozzle ...
THERMAL SCIENCE: Year 2019, Vol. 23, No. 4, pp. 2143-2150

2147

collector when the collector speed increases to 80 mm per second as shown in figs. 4(d) and 4(e).

On the other hand, the jet can be regarded as an incompressible viscous Newtonian fluid in the process of NFES direct-writing. Hence, gravity, g, the interaction of the electric field force, F_e, Coulomb force, F_C, viscosity force, F_v, and electrodeposition force, F_{ed}, are forced during the jetting process and electric field force and coulomb force occupy the main role in this process. The force of the rheological process of the jet can be described:

$$\rho \frac{du}{dt} = g + F_e + F_C + F_{ed} + F_v \qquad (4)$$

where u is the axial speed of the jet, ρ – the volume charge density, and du/dt is the material derivative [24].

The volume charge density of the jet becomes smaller as the applied voltage decreasing, and whose electric field strength becomes weaken. The driving force of the Taylor cone at the needle become weaken, resulting in a mismatch between the voltage and the solution supply speed. In other words, the stability of the jet gets deteriorated and the greater traction is needed to overcome the instability of the jet on the same collector. However, the jet speed is proportional to the traction force in the NFES direct-writing deposition process, so the role of the jet at low voltage requires a higher speed to rebalance the motion. Therefore, it can be further confirmed that the critical speeds of the collector in the NFES aligned nanofibers are 80 mm per second and 15 mm per second when the operating voltages are $U = 1.5$ KV and 2.5 KV, respectively.

Because the fiber electrospinning speed and the collector speed can be regarded as consistent in the NFES deposition process, ignoring the volatilization effect during the flight of the jet. By eq. (4), the applied voltage is a positive relationship on the diameter of nanofibers as shown in fig. 5. The flow rate of the solution deposited on the collector and the diameter of nanofibers increases with the solution feed rate as the enhanced driving effect of the high-voltage electric field on the jet.
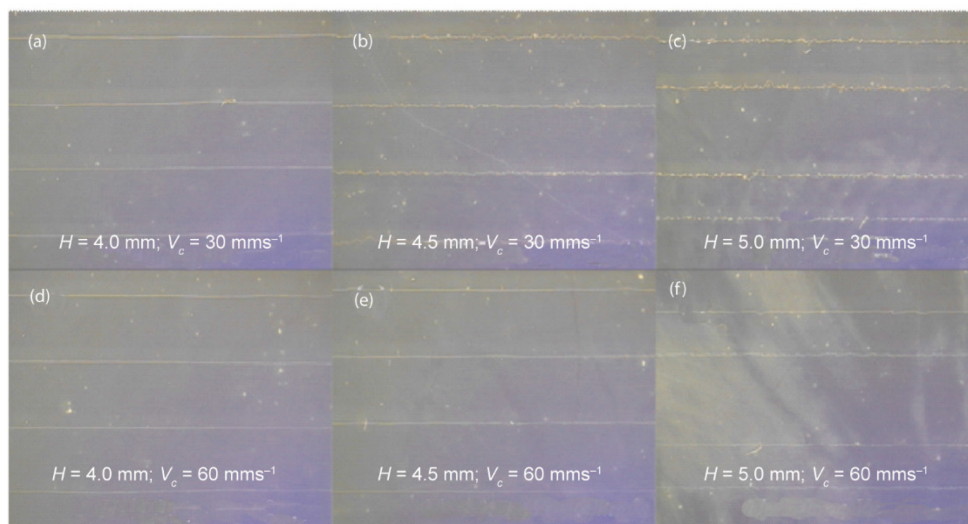
Effect of electrode-to-collector distance on the direct-write deposition structure

The electrode-to-collector distance will affect electric field intensity. As shown in figs. 6 and 7, the average diameter of nanofibers is negative correlated with the electrode-to-collector distance.

The critical speed of the collectors for the NFES aligned pattern is 30, 60, and 80 mm per second when the working polar distances are 4.0, 4.5, and 5.0 mm, respectively. On the other hand, the electrode-to-collector distance and the applying voltage during the spinning process are similar to the electric field strength, the distribution of the ES environment will be directly affected by the previous parameters. Therefore, the electric field intensity near the needle tip decreases with the electrode-to-collector distance arising, causing the deposition time of the jets to elongate and the jet will stretch to be finer and longer whose average diameter become smaller during the same deposition process. Moreover, a larger speed is required to maintain the aligned pattern with the increasing rate of the deposition jet.

Conclusions

In this paper, a comprehensive study is carried out to explore the effect of the relationship between the parameters (collector speed, applied voltage, and electrode-to-collector dis-

Figure 6. The jets deposition pattern at different electrode-to-collector distance in the condition with 0.5 inch needle length, 2.0 mm needle space, 2.0KV applied voltage
(*for color image see journal web site*)
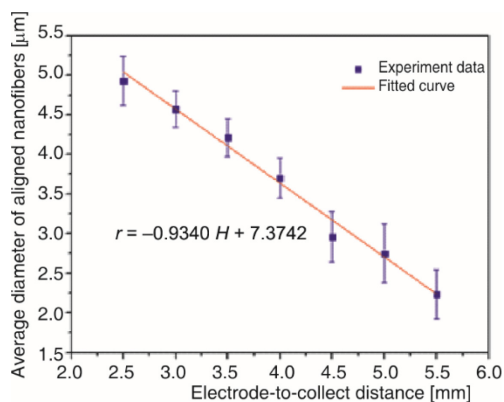
Figure 7. The average diameter of aligned nanofibers at different electrode-to-collector distance

tance) and the deposition morphology in the process of double-nozzle NFES to fabricate aligned nanofibers. The following conclusions are drawn from the experiment.

- Collector speed has a significant effect on the aligned nanofibers. Bead shape will appear when the speed is low enough. However, deposition pattern changes from beaded fibers to crimpled fibers, and finally to aligned line as the speed increases. At the same time, the diameter of the deposition aligned nanofibers shows a negative trend of the power function: $r = -4.5725u^{0.1344} + 10.6857$.

- The deposition of aligned nanofibers is straighter as the voltage increases. Meanwhile, the diameter of nanofibers also increases linearly when the voltage increases within a certain voltage range.

- The electrode-to-collector distance has not a significant effect on the aligned nanofibers, and the direct-write deposition shows a tendency to turn linearly as the electrode-to-collector distance reduces.

Acknowledgment

Xu, G., *et al.*: Accurate Fabrication of Aligned Nanofibers *via* a Double-Nozzle …
THERMAL SCIENCE: Year 2019, Vol. 23, No. 4, pp. 2143-2150

2149

Nomenclature

F_C – Coulomb force, [N]
F_e – electric field force, [N]
F_{ed} – electrodeposition force, [N]
F_v – viscosity force, [N]
g – gravity, [N]
H – electrode-to-collector distance, [mm]
r – jet diameter, [mm]
U – applied voltage, [kV]

u – axial speed of the jet, [mms^{-1}]
V_c – collector speed, [mms^{-1}]
v_f – fiber electrospinning speed, [mms^{-1}]
V_f – flow rate, [μm per minute]

Greek symbol

ρ – volume charge density, [Cm^3]

References

[1] Balen, R., *et al.*, Structural, Thermal, Optical Properties and Cytotoxicity of PMMA/ZnO Fibers and Films: Potential Application in Tissue Engineering, *Applied Surface Science, 385* (2016), Nov. pp. 257-267
[2] Chang, J. H., *et al.*, A Solution-Processed Molybdenum Oxide Treated Silver Nanowire Network: a Highly Conductive Transparent Conducting Electrode with Superior Mechanical and Hole Injection Properties, *Nanoscale, 7* (2015), 10, pp. 4572-4579
[3] Jeong, U., *et al.*, Chemical Transformation: a Powerful Route to Metal Chalcogenide Nanowires, *Cheminform, 38* (2007), 9, pp. 3893-3897
[4] Kim, J. Y., *et al.*, Flexible and Transferrable Self-Assembled Nanopatterning on Chemically Modified Graphene, *Advanced Materials, 25* (2013), 25, pp. 3396-3396
[5] Min, S. Y., *et al.*, Organic Nanowire Fabrication and Device Applications, *Small, 11* (2015), 1, pp. 45
[6] Pinto, N. J., *et al.*, Electrospun Polyaniline/Polyethylene Oxide Nanofiber Field Effect Transistor, *Applied Physics Letters, 83* (2003), 20, pp. 4244-4246
[7] Zeng, J., *et al.*, Fabrication of Microfluidic Channels Based on Melt-Electrospinning Direct Writing, *Microfluidics and Nanofluidics, 22* (2018), 2, 23
[8] Liu, Z., R. *et al.*, Active Generation of Multiple Jets for Producing Nanofibres with High Quality and High Throughput, *Materials & Design, 94* (2016), Mar., pp. 496-501
[9] Huang, H., *et al.*, Crimp Frequency of a Viscoelastic Fiber in a Crimping Process, *Thermal Science, 21* (2017), 4, pp. 1839-1842
[10] Huang, J. X., *et al.*, Transverse Vibration of an Axially Moving Slender Fiber of Viscoelastic Fluid in Bubbfil Spinning and Stuffer Box Crimping, *Thermal Science, 19* (2015), 4, pp. 1437-1441
[11] He, X. X., *et al.*, Near-Field Electrospinning: Progress and Applications, *Journal of Physical Chemistry C, 121* (2017), 16, pp. 8663-8678
[12] Sun, D. H., *et al.*, Near-Field Electrospinning, *Nano Letters, 6* (2006), 4, pp. 839-842
[13] Fuh, Y. K., *et al.*, The Control of Cell Orientation Using Biodegradable Alginate Fibers Fabricated by Near-Field Electrospinning, *Materials Science & Engineering C Materials for Biological Applications, 62* (2016), May, pp. 879-887
[14] Fuh, Y. K., *et al.*, Hybrid Energy Harvester Consisting of Piezoelectric Fibers with Largely Enhanced 20 V for Wearable and Muscle-Driven Applications, *Acs. Applied Materials & Interfaces, 7* (2015), 31, pp. 16923–16931

2150

Xu, G., *et al.*: Accurate Fabrication of Aligned Nanofibers *via* a Double-Nozzle …
THERMAL SCIENCE: Year 2019, Vol. 23, No. 4, pp. 2143-2150

[15] Liu, Z. H., *et al.*, Crystallization and Mechanical Behavior of the Ferroelectric Polymer Nonwoven Fiber Fabrics for Highly Durable Wearable Sensor Applications, *Applied Surface Science, 346* (2015), Aug., pp. 291-301

[16] Wang, X., *et al.*, Fabrication of Nanochannels via Near-Field Electrospinning, *Applied Physics A, 108* (2012), 4, pp. 825-828

[17] Chang, C., *et al.*, Direct-Write Piezoelectric Polymeric Nanogenerator with High Energy Conversion Efficiency, *Nano Letters, 10* (2010), 2, pp. 726-731

[18] Bellan, L. M., Craighead, H. G., Nanomanufacturing Using Electrospinning, *Journal of Manufacturing Science & Engineering, 131* (2009), 3, pp. 337-346

[19] Brown, T. D., *et al.*, Direct Writing by Way of Melt Electrospinning, *Advanced Materials, 23* (2011), 47, pp. 5651-5657

[20] Varesano, A., *et al.*, Experimental Investigations on the Multi-Jet Electrospinning Process, *Journal of Materials Processing Tech, 209* (2009), 11, pp. 5178-5185

[21] Zheng, G., *et al.*, Self-Cleaning Threaded Rod Spinneret for High-Efficiency Needleless Electrospinning, *Applied Physics A, 124* (2018), 7, ID 473

[22] Pan, Y., *et al.*, Fabrication of Si-Nozzles for Parallel Mechano-Electrospinning Direct Writing, *Journal of Physics D Applied Physics, 46* (2013), 25, ID 255301

[23] Wang, Z., *et al.*, Controllable Deposition Distance of Aligned Pattern via Dual-Nozzle Near-Field Electrospinning, *Aip Advances, 7* (2017), 3, ID 035310

[24] Wang, H., *et al.*, Deposition Characteristics of the Double Nozzles Near-Field Electrospinning, *Applied Physics A, 118* (2014), 2, pp. 621-628